

Utah State University

DigitalCommons@USU

---

Senior Theses and Projects

Materials Physics

---

3-2016

## Developing a Safe Test System for High-energy Electron Flux Environments Testing

Heather Tippetts

*Brigham Young University Idaho*

Follow this and additional works at: [https://digitalcommons.usu.edu/mp\\_seniorthesesprojects](https://digitalcommons.usu.edu/mp_seniorthesesprojects)



Part of the [Condensed Matter Physics Commons](#)

---

### Recommended Citation

Tippetts, Heather, "Developing a Safe Test System for High-energy Electron Flux Environments Testing" (2016). *Senior Theses and Projects*. Paper 24.

[https://digitalcommons.usu.edu/mp\\_seniorthesesprojects/24](https://digitalcommons.usu.edu/mp_seniorthesesprojects/24)

This Report is brought to you for free and open access by the Materials Physics at DigitalCommons@USU. It has been accepted for inclusion in Senior Theses and Projects by an authorized administrator of DigitalCommons@USU. For more information, please contact [digitalcommons@usu.edu](mailto:digitalcommons@usu.edu).



# Radiation Safety Design for High Energy Electron Flux Environments Testing

By

Heather Tippets

A senior thesis submitted to the faculty of

Brigham Young University – Idaho

In partial fulfillment of the requirements for the degree of

Bachelor of Science

Department of Physics

Brigham Young University – Idaho

March 2016

Copyright © 2016 Heather Tippetts

All Rights Reserved

BRIGHAM YOUNG UNIVERSITY – IDAHO

DEPARTMENT APPROVAL

of a senior thesis submitted by

Heather Tippets

This thesis has been reviewed by the research committee, senior thesis coordinator, and department chair and has been found to be satisfactory.

\_\_\_\_\_  
Date

\_\_\_\_\_  
Todd Lines, Advisor

\_\_\_\_\_  
Date

\_\_\_\_\_  
David Oliphant, Committee Member

\_\_\_\_\_  
Date

\_\_\_\_\_  
Kevin Kelley, Committee Member

\_\_\_\_\_  
Date

\_\_\_\_\_  
Evan Hansen, Committee Member

\_\_\_\_\_  
Date

\_\_\_\_\_  
Stephen McNeil, Department Chair

## ABSTRACT

### Radiation Safety Design for High Energy Electron Flux Environments Testing

Heather Tippets

Department of Physics

Bachelor of Science

In order to predict and mitigate adverse environmental effects on spacecraft in orbit about Earth, a versatile pre-launch test capability for assessment and verification of small satellites, systems, and components was developed by Utah State University's Materials Physics Group. To further diversify this project, a 100 mCi Sr-90 beta radiation source (0.5 MeV – 2.5 MeV) is exploited to simulate the high energy electron flux of geostationary orbit. Various samples including in-the-loop hardware, spacecraft materials, optical components, and solar arrays are irradiated to gain a better understanding of how these materials and electronics break down in space environments. For employee protection, various high and low-Z shielding materials were implemented near the test chamber to minimize X-ray dose rates. In order to forecast employee dose while working around the source, X-ray attenuation through the various shielding materials was calculated. Upon discovering a deficiency in shielding capability,

additional lead shielding was implemented to lower dose rates outside of the test chamber to nearly background. Prediction of attenuated dose rates strongly correlate with actual measurements post source installation.

## Acknowledgements

I would like to express my sincerest thanks to my research mentor Dr. JR Dennison for the support of my internship with Utah State University. His guidance, patience, and savvy advice provided me with a memorable research experience and was an aid in the process of writing this thesis.

I would also like to thank my thesis advisor Dr. Todd Lines and my thesis committee: Dr. David Oliphant, Dr. Evan Hansen, and Dr. Kevin Kelley for their encouragement and insightful suggestions.

A special thanks to the BYU-Idaho Physics Department and faculty for giving me opportunities to grow in knowledge, confidence, and humility.

Thank you to my family, for encouraging me to pursue a fullness of life and to do hard things with optimism.

Lastly, to my sweet husband, for his love and constant support.

# Table of Contents

<b>INTRODUCTION</b> .....	<b>ERROR! BOOKMARK NOT DEFINED.</b>
1.1 IONIZING RADIATION .....	2
1.2 METHOD OF SIMULATING GEO .....	2
1.3 SAMPLE PLATE DESIGN CONSIDERATIONS .....	3
1.4 SHIELDING.....	4
<b>MIMICKING HIGH ENERGY GEOSTATIONARY ORBIT ELECTRON SPECTRA.....</b>	<b>5</b>
2.1 SOLAR WIND ELECTRON RADIATION IN LOW EARTH/GEOSTATIONARY ORBITS .....	5
2.2 THE SPACE SURVIVABILITY TEST CHAMBER .....	6
2.3 HIGH ENERGY ELECTRON RADIATION SIMULATED WITH SR-90 SOURCE .....	<b>ERROR! BOOKMARK NOT DEFINED.</b>
<b>PROCEDURES AND METHODS FOR PREDICTING SHIELDING AND DOSE RATES.....</b>	<b>9</b>
3.1 UNITS OF DOSE.....	9
3.2 DOSE LIMITS .....	11
3.3 SR-90 SOURCE HOUSING AND SHIELDING DESING.....	11
3.4 RADPRO CALCULATOR.....	14
3.5 SCATTERING LENGTH AND X-RAY ATTENUATION OF MATERIALS.....	15
<b>RESULTS AND ANALYSIS .....</b>	<b>20</b>
4.1 ACCUMULATED DOSE SCENARIO .....	20
4.2 THEORETICAL VERSUS EXPERIMENTAL DOSE RATES.....	21
4.3 ERROR ANALYSIS.....	23
4.3.1 DOSE RATE EQUATION.....	23
4.3.2 STANDARD DEVIATION OF ATTENUATED DOSE RATE.....	24
4.3.3 CALCULATING $\chi^2$ .....	26
<b>CONCLUSION.....</b>	<b>28</b>
<b>BIBLIOGRAPH .....</b>	<b>29-31</b>

# List of Figures

1.1 Common electron flux environments.....	2
1.2 Sample Plate.....	3
2.1 Space Survivability Test (SST) chamber.....	7
3.1 Sr-90 Source Housing Design.....	12
3.2 Cross sectional of source housing.....	13
3.3 X-ray intensity attenuation.....	15
3.4 X-ray attenuation of shielding materials.....	17
4.1 Measured vs Predicted Attenuated Dose Rates.....	22
4.2 Predicted Attenuated Dose Rates.....	26

# List of Tables

1.1 Density of Shielding Materials.....	4
3.1 Basic conversions between units of dose.....	10
3.2 Scattering lengths of shielding materials.....	16
3.3 Thickness of shielding materials.....	18
3.4 Preliminary dose rates calculated by RadPro Calculator.....	19

# Chapter 1

## Introduction

Utah State University's Materials Physics Group (MPG) has developed a versatile ground-based testing capability to simulate space-like environments from low earth orbit (LEO) to geostationary orbit (GEO) [1]. In particular, I was involved with simulating the electron flux of GEO. Using a series of high and low energy electron guns, the MPG developed an electron flux capability with a range of 10 eV to 50 keV. This range mimics environments such as low earth orbit (LEO), auroral maximums, solar wind, and the plasma sheet in our upper atmosphere. To extend this capability to include testing of radiation damage caused by higher energy electron flux such as that found in GEO, a 100 mCi strontium-90 beta emitter was installed.

### **1.1 Ionizing Radiation**

Ionizing radiation is a flux of charged particles such as electrons ( $\beta$ ), protons (p), alphas particles ( $\alpha$ ), gamma rays ( $\gamma$ ), or fission fragments. This type of radiation can damage sensitive electronics and degrade materials. As electrons pass through matter, they strongly interact with the material's orbital electrons and several possible processes can occur: ionization of the material, elastic scattering, or production of bremsstrahlung

emission, which is the creation of X-rays from a rapid change in the momentum of electrons. Electrons can also penetrate through materials and can cause atomic displacement. The distance they penetrate depends on the density of the material and the speed of the electron.

## 1.2 Method of Simulating GEO

Variation of electron fluxes in geostationary orbit is largely affected by solar wind speed and can fluctuate daily [2]. A strontium-90 (Sr-90) beta radiation source was chosen to simulate the average peak electron spectra in geostationary orbit (GEO). The source has an energy spectra of 0.5 MeV – 2.5 MeV and simulates GEO environment at 4 to 10 times accelerated rates. Figure 1.1 shows representative electron spectra for several common environments.

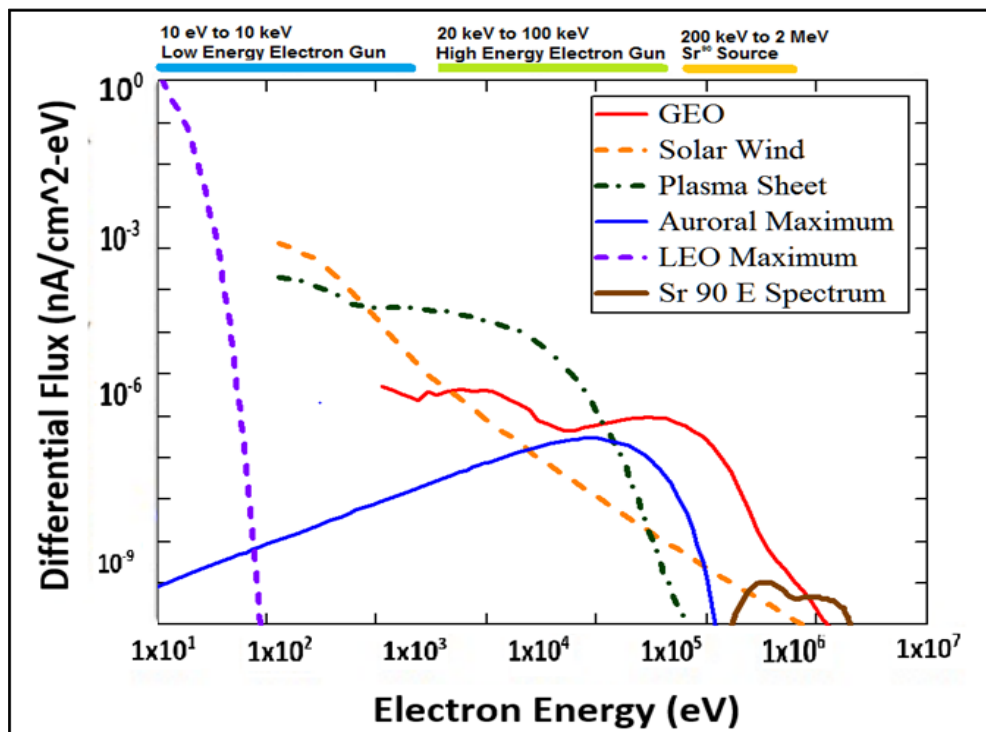


**Figure 1.1** Common electron flux environments relevant to LEO through GEO. A Sr-90 source mimics the higher end of the GEO electron energy spectrum [8].

Due to the high activity of the source (100 mCi), it was crucial that the environment outside of the test chamber be effectively shielded. The Sr-90 source could not legally be installed until proper shielding was proven to attenuate the dose rates exiting the chamber to legal limits. My primary responsibility was to calculate these attenuated dose rates and predict employee dose while working around the shielded source. In order to accomplish this, I calculated the X-ray attenuation through each shielding material and developed an accumulated dose rate scenario that describes the expected employee dose.

### 1.3 Sample Plate Shielding Considerations

The purpose the Sr-90 source is to irradiate materials, components, and systems that would be used on satellites and spacecraft to determine how they break down in orbit

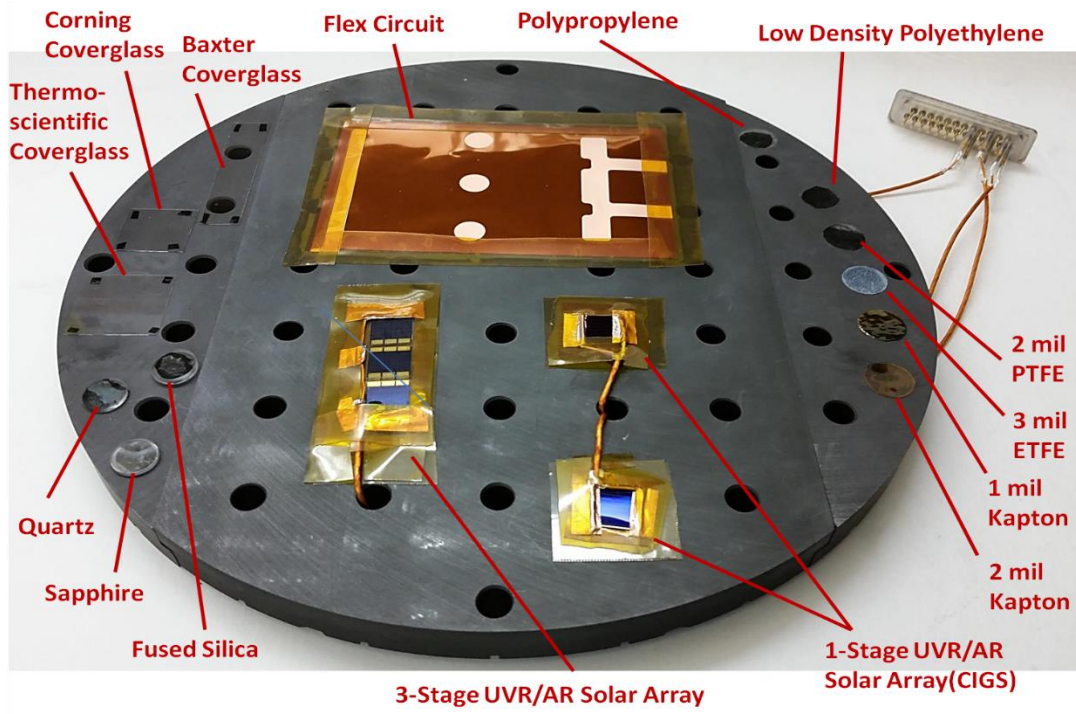


**Figure 1.2** Sample plate with various optical, materials, and electrical samples attached.

about earth. A rotatable sample plate holds various polymers, cover glasses and optical components common to small satellites, flexible circuits, solar arrays, and materials used on spacecraft such as kapton and mylar (Figure 1.2). The polytetrafluoroethylene (PTFE) samples serve as a calibration constant. These same samples were exposed to low earth orbit while flying on the MISSE-6 mission [11]. They will determine how well the test chamber simulates actual space environment. The sample plate is made of layers of graphite and stainless steel for shielding purposes.

## 1.4 Shielding

As the Sr-90 beta source irradiates samples in the test chamber, some of the electrons from the beam of radiation collide with high density shielding materials and produce X-rays. Shielding beta particles requires a series of low and high-Z moderators. Low-Z materials absorb beta radiation well. However, if an electron collides directly with a high-Z material, X-rays will be produced. The shielding materials used for beta particles and X-rays and their relative densities are listed in Table 1.1

**Table 1.1** Shielding materials for electron and X-ray radiation and their relative densities

MATERIAL	DENSITY ( $g/cm^3$ )
Graphite (C)	2.26
Aluminum (Al)	2.7
Copper (Cu)	8.9
Stainless steel (Fe)	7.87
Lead (Pb)	11.8
Tungsten (W)	19.25

# Chapter 2

## Mimicking the High Energy Geostationary Orbit Electron Spectra

Spacecraft and satellites orbiting Earth experience a broad electron flux from solar wind. Simulation capabilities of the Space Survivability Test (SST) permit accelerated ground-based testing of environmentally-induced modifications to materials and components. A Sr-90 beta radiation source approximately mimics the geostationary high energy electron spectra at 4 to 10 times accelerated rates. The Sr-90 source serves to forecast sample radiation damage, predict the lifetime of electronics, and diversify the ability of the SST chamber to simulate space environment.

### **2.1 Solar wind electron radiation in Low Earth/Geostationary Orbits**

Solar wind is the continuous flow of high energy electrons, protons and free ions ejected from the sun. The outermost layer of the solar atmosphere, known as the corona, contains holes where the magnetic field lines of the sun are open. These coronal holes blast streams of energized, charged particles outward into the solar system at high speeds. Although Earth's magnetosphere protects our planet from most solar radiation, a small portion of highly energized electrons and protons still make it through to Earth's upper atmosphere. Spacecraft in LEO through GEO undergo significant electron flux from solar

wind. Electron radiation can cause damage to sensitive electronics, alter optical properties, deteriorate components, and reduce the overall lifetime of satellites and spacecraft [9]. Electrons have very low mass and can be given a large energy when ejected from coronal holes. Protons, however, are much more massive than electrons, and thus rarely reach speeds that could significantly penetrate and damage electronics on satellites. Fast moving protons can be a significant source a damage, even though they exhibit very low fluxes in LEO/GEO. Proton accelerators are incredibly expensive, however, and so the Materials Physics Group (MPG) was limited to using only electron flux sources.

## **2.2 The Space Survivability Test Chamber**

The Space Survivability Test (SST) chamber is a versatile accelerated ground-based test facility designed to simulate environmental-induced modifications in LEO and GEO. Simulation capabilities include neutral gas atmosphere and vacuum environments ( $< 10^{-6} \text{ Torr}$ ), temperature ( $\sim 60 \text{ K} - 450 \text{ K}$ ), ionizing radiation, electron fluxes ( $\sim 10 \text{ eV} - 2.5 \text{ MeV}$ ), and photon fluxes ranging from far-ultraviolet to near-infrared (FUV/VIS/NIR). This versatile test chamber is particularly suited for the testing of complete systems ( $< 20 \text{ cm diameter}$ ) such as 1U CubSats, commercial-off-the-shelf components (COTS), electronics, and individual material samples. The SST can perform multiple *in-situ* radiation and environments tests simultaneously, as well as facilitate ex-situ tests before and after exposure. The Strontium-90 Test (SRaT) chamber is an attachment to the SST chamber that holds the Sr-90 source housing. An airline actuator

rod allows the Sr-90 source housing to slide out of the SRaT chamber and into the SST chamber to irradiate samples.

## Space Survivability Test (SST) chamber

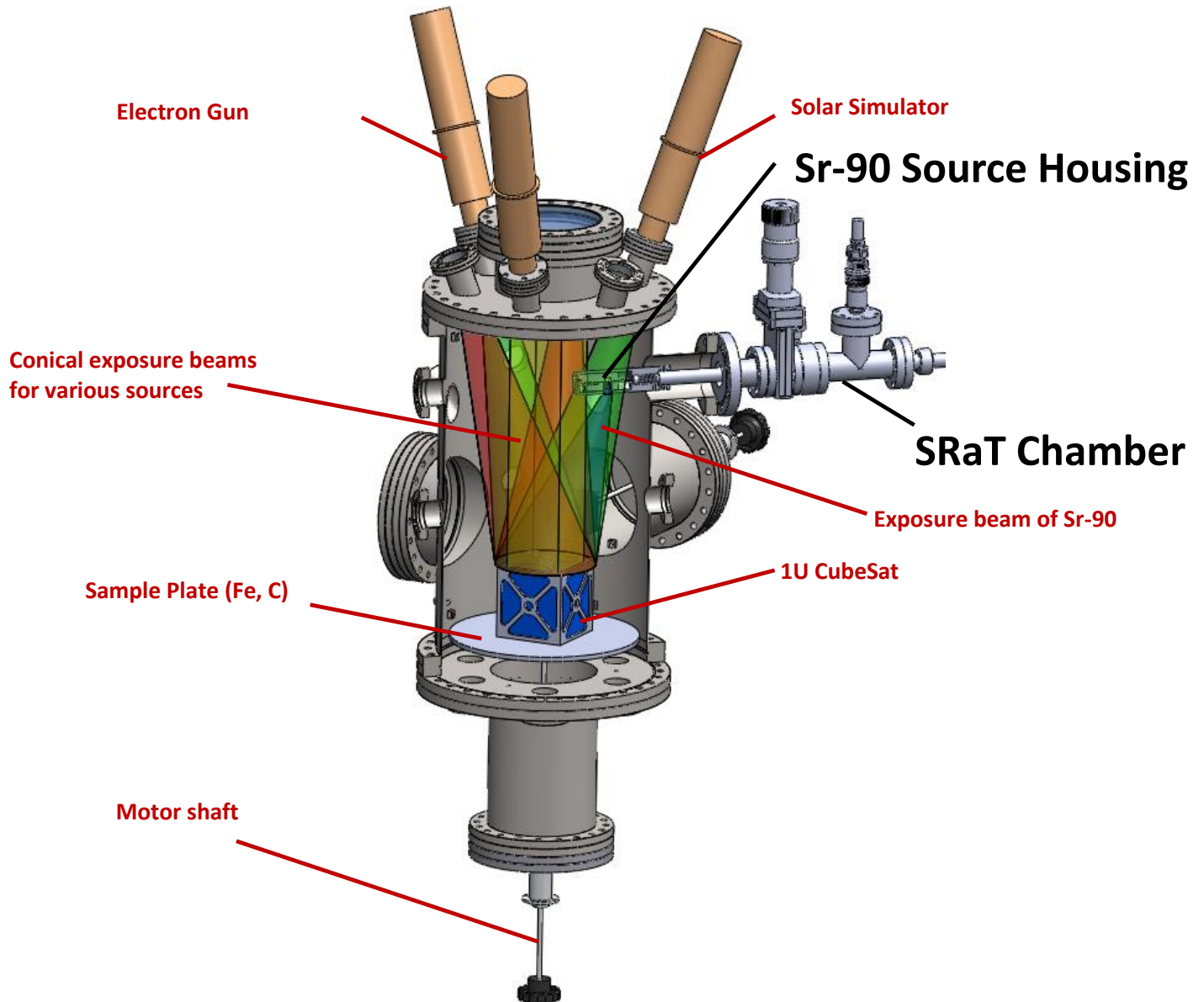


**Figure 2.1** Space Survivability Test (SST) chamber and Strontium-90 Test (SRaT) chamber with various simulation capabilities attached [7].

### **2.3 High energy electron radiation simulated with Sr-90 source**

In order to predict and mitigate environmental-induced corrosion of spacecraft and satellites due to radiation damage, a safe radiation test system was designed to simulate the higher end of the GEO electron spectra (0.2 MeV – 2 MeV). A 100 mCi Strontium-90 beta radiation source approximately mimics the high energy electron spectra. The source has an emission energy of 0.2 MeV- 2 MeV which resembles a range of the electron spectrum found in GEO. The Sr-90 source was installed in the SST chamber to irradiate various materials, electronics, and components in order to forecast radiation damage, predict the lifetimes of electronics, and authenticate the ability of the test chamber to mimic space environment.

## Chapter 3:

# Procedures and Methods for Predicting Shielding and Dose Rates

This section will discuss the shielding designed to keep employees protected from harmful radiation while working around the Strontium-90 source. Units of dose and dose limits will be introduced. The strontium-90 source housing and shielding design will be covered in detail to illustrate how the shielding calculations were carried out. Scattering lengths of various shielding materials were calculated and used to predict X-ray attenuation distances in those materials. Additional shielding was installed after discovering a deficiency in shielding capability for certain orientations around the test chamber. Dose rates were predicted for various orientations around the source in both storage and exposure positions.

### **3.1 Units of Dose**

X-rays produced by excited electrons in the Strontium-90 Test chamber (SRaT) and Space Survivability Test chamber (SST) posed a potential threat to employees. High-energy radiation, such as X-rays, can cause damage to human tissue. The amount of

radiation and time of exposure are key to determining how significant the dose is. What is known about radiation strongly suggests that getting a certain dose in a short period of time is significantly more serious than getting the same dose over a long period of time. In order to make sure that employees were safe during installation and use of the Sr-90 source, my first priority was to predict the amount of dose that would theoretically be leaking out of the chamber if the source was inside.

Units of dose can often be confusing, namely because there are so many of them. The raw physical units that describe radiation emitted by a radioactive material are curies (Ci) and becquerels (Bq). A becquerel is equal to one decay per second, and a curie is equal to  $3.7 \times 10^{10}$  Bq. Units that describe the amount of energy absorbed by a mass are measured in rad or gray (Gy). Relative biological damage is measured in units of rem or sieverts (Sv), and depends on the type of radiation. Gamma rays and X-rays are less damaging to tissue than large particle radiation, such as alpha particles [4]. With respect to X-rays and gamma rays, one rem is equivalent to one rad. I will consistently use units of rads throughout this paper. A table of basic conversions between these units is listed in Table 3.1 below.

**Table 3.1** Basic conversions between units of dose

UNIT	EQUIVALENT
1 gray (Gy)	100 rad
1 sievert (Sv)	100 rem
1 becquerel (Bq)	1 count per second (cps)
1 curie (Ci)	37,000,000,000 Bq
For X-rays and gamma rays:	
1 rad	1 rem, 10 mSv

### **3.2 Dose limits**

The dose limits for radiation workers are established in the *Code of Federal Regulations (10 CFR Part 20)*, "Standards for Protection Against Radiation". The annual total effective dose equivalent (TEDE) for the whole body is 5,000 mrem (5 rem). For extremities and skin, the annual legal limit is 50 rem. For the eyes, the annual limit is 15 rem. Some tissues are more radiosensitive than others, meaning that they are more prone to radiation damage. Cells that have large nuclei, divide quickly, or are well nourished are more radiosensitive. Extremities are less radiosensitive than large internal organs, and thus have a higher dose limit.

### **3.3 Sr-90 Source Housing and Shielding Design**

The Sr-90 source has an activity of 100 mCi and produces a dose rate of approximately 800 rad/hr directly above the unshielded face of the source. If direct contact was made with this source, an individual would receive their total annual whole body dose limit in about 22 seconds. Because of the high dose rate given off by this source, it was necessary to determine if the current shielding capability in these chambers was sufficient to allow employees and students to safely carry out experiments around the source. Additional concerns were considered for the process of assembling the Sr-90 source into the chamber.

The Sr-90 source is a chemically bound ceramic active element, and is enclosed in a weld-sealed capsule. A thin stainless steel window rests on top of the active side of the source, and a composite shielding structure encapsulates the sides and bottom of the source. The primary radiation is emitted from the front surface (active side) of the Sr-90 capsule through the stainless steel window. This encapsulated source is mounted in a custom designed housing (Figure 3.1). The housing incorporates graphite, tungsten and stainless steel shielding. The source is mounted in a half-cylinder of tungsten. The source

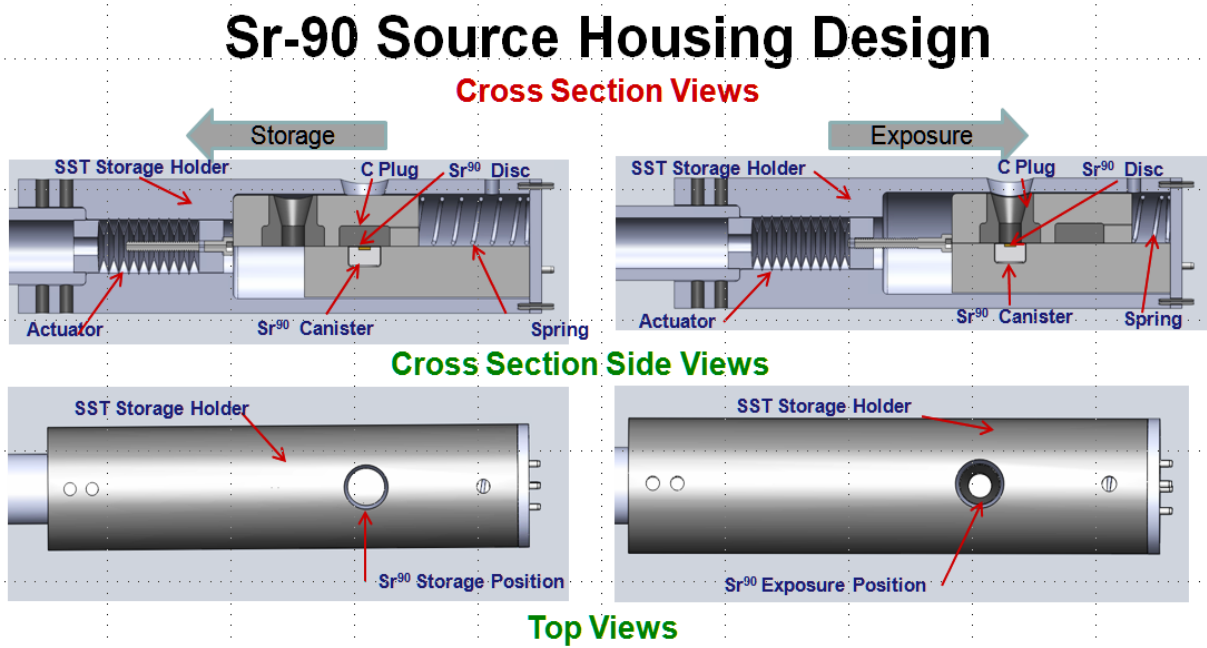


**Figure 3.1** Sr-90 source housing design. (Top) Source cross section views with source in storage (left) and exposure (right) positions. (Bottom) Exterior views from top showing source in storage (left) and exposure (right) positions.

housing has a movable shutter which allows (i) a fail-safe storage position and (ii) an exposure position. The shutter is moved to the exposure position using a pneumatic controlled actuator, and returned to the fail-safe storage position with a spring. In Figure 3.2, the sealed source is in the storage position and surrounded by a low-Z beta radiation moderator (graphite) of more than sufficient thickness to stop electron radiation from leaking out of the chamber. The graphite is surrounded by a high-Z shielding layer of tungsten (W) to attenuate the bremsstrahlung radiation produced in the low-Z moderator.

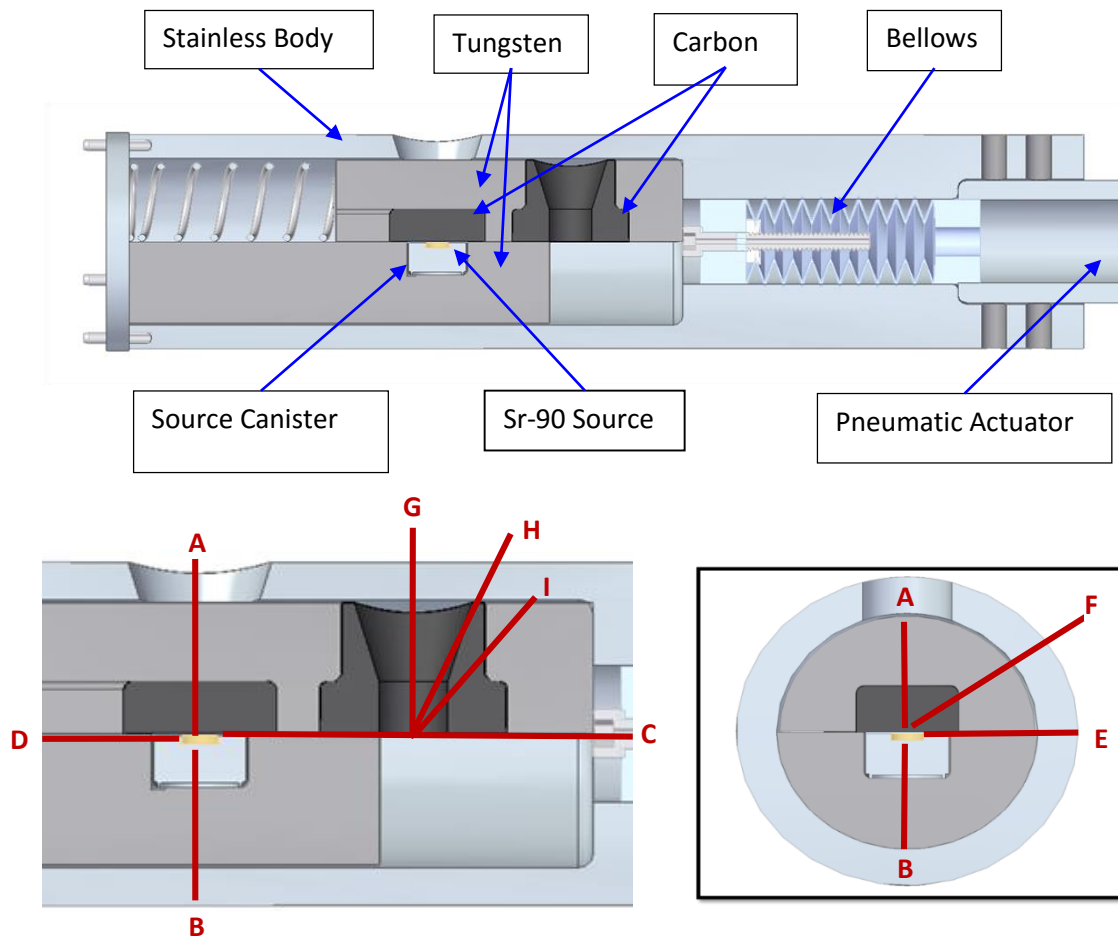


**Figure 3.2** (Top) source housing shielding design. (Bottom) Cross section of various paths through shielding materials. **A** – Storage position, in direction of radiation beam, **B** – Opposite the beam of radiation, **C** – Towards the actuator rod. **D** – Toward the housing end cap, **E** – In the plane of the Sr-90 source, directly outward from the housing, **F** – 45° from the plane of Sr-90 source, **G** – Exposure position, **H** – 15° from exposure position, **I** – 45° from exposure position

This is further packaged in a stainless steel tube.

### 3.4 RadPro Calculator

I calculated the X-ray dose rate from the Sr-90 source along each path in Figure 3.2 for both the storage and exposure positions. These are the preliminary dose rates exiting the source housing. The calculations were made using a Rad Pro Calculator software package (Version 3.26). This software predicts dose rates from a radioactive source through various shielding materials. While using this software, I chose the radiation type to be Sr-90/Y-90. This option simulates the decay of strontium-90 into yttrium-90. Sr-90 has a half-life of about 29 years. Yr-90 has a half-life of 64 hours and makes up about 5% of the daughter isotopes, Yr-90 decays into zirconium-90, which is stable. Using Sr-90/Y-90 in the Rad Pro Calculator software is a good approximation for our Sr-90 source.

The radiation activity was set to 100 mCi. Low density polyethylene (LDPE) was chosen as a proxy material in lieu of graphite for the beta shielding material. LDPE has a density  $0.88 \frac{g}{cm^3}$  while graphite has a density  $2.2 \frac{g}{cm^3}$ . Assuming the beta shielding scales as the density, the graphite will give about 2.5 times the beta shielding as that predicted with the software using LDPE. However, since the beta shielding predicted by the Rad Pro Calculator was essentially complete in all cases, this had little effect on the radiation calculations performed. X-ray shielding materials and their thickness were also input into the software. These materials included stainless steel, tungsten, lead, aluminum, and copper.

### 3.5 Scattering Length and X-ray Attenuation of Materials

Radiation decreases in intensity as it moves through a substance due to its interaction with matter. The attenuation properties of materials, such as thickness and density, will determine the type and magnitude of shielding materials necessary to block radiation, as well as how much dosage one receives. Radiation that has a short scattering length attenuates quickly and will have a higher dosage near the surface of the shielding materials. Radiation that has a long scattering length attenuates slowly and loses its energy over a long distance; thus, it will carry a lower dosage. To calculate the X-ray

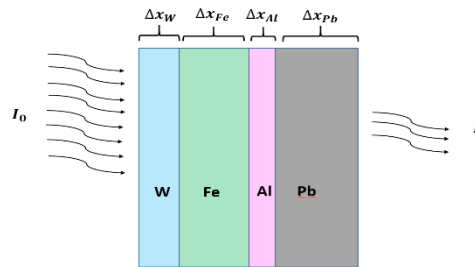


**Figure 3.3** X-ray intensity attenuates through shielding materials. Attenuation depends on the thickness and density of the material.

dose rate exiting the source housing, the thicknesses of all the shielding materials were first measured. The scattering lengths were then calculated through each of these materials for the minimum energy (0.5 MeV) and maximum energy (2.5 MeV) of electron radiation from the Sr-90 source. The shielding materials include tungsten (W), stainless steel (Fe), and aluminum (Al) (Figure 3.3). Later in this chapter, the addition of lead shielding added due insufficient shielding from these other materials will be discussed.

The initial X-ray intensity  $I_0$  attenuates as it passes through a shielding material with some thickness  $x$ . The number of X-rays that pass through a slab of material decreases exponentially with thickness:

$$I(x) = I_0 e^{-\alpha x} = I_0 e^{-\frac{x}{L}} \quad (1)$$

This equation is referred to as Lambert's law and applies to linear attenuation.  $\alpha$  is the linear attenuation coefficient,  $L$  is the scattering length, and  $x$  is the thickness of the material. Scattering length is calculated by

$$L = \frac{1}{\mu\rho} \quad (2)$$

where  $\mu$  is the mass attenuation coefficient and  $\rho$  is the density of the material. The product  $\mu\rho$  is the linear attenuation coefficient  $\alpha$ . The scattering lengths for each shielding material are listed in Table 3.4 for both the 0.5 MeV X-rays and the 2.5 MeV X-rays.

**Table 3.2** Scattering lengths for shielding materials for (top) 0.5 MeV and (bottom) 2.5 MeV X-rays.

MATERIAL	$\mu \left( \frac{cm^2}{g} \right)$	$\rho \left( \frac{g}{cm^3} \right)$	$L (cm)$
Pb	0.14	11.8	0.61
Cu	0.085	8.9	1.3
Al	0.082	2.7	4.5
W	0.13	19.25	0.4
Fe	0.082	7.87	1.5

MATERIAL	$\mu \left( \frac{cm^2}{g} \right)$	$\rho \left( \frac{g}{cm^3} \right)$	$L (cm)$
Pb	0.042	11.8	2.0
Cu	0.040	8.9	2.8
Al	0.040	2.7	9.3
W	0.041	19.25	1.3
Fe	0.037	7.87	3.4

With these predicted scattering lengths, the attenuation factor  $\xi$  was then calculated through each material. The attenuation factor simply represents the percent of radiation that gets through the material. Multiplying the preliminary dose rates (calculated by Rad Pro calculator) by this attenuation factor gives the attenuated dose rate being emitted through a shielding material. The equation for the linear attenuation factor is

$$\xi = \frac{I(x)}{I_0} = e^{-\frac{x}{L}} \quad (3)$$

The attenuation factor for each shielding material for both minimum energy (0.5 MeV) and maximum energy (2.5 MeV) is shown below in Figure 6.

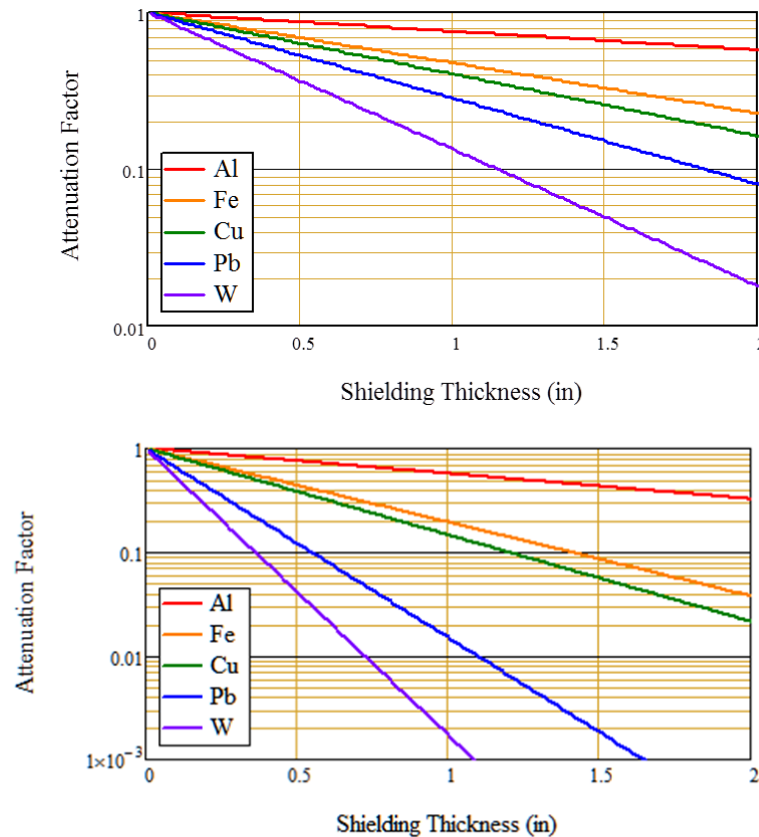


**Figure 3.4** X-ray attenuation for relevant materials at 2.5 MeV (top) and 0.5 MeV (bottom)

The calculations for the attenuated dose rates emitted around the SRaT chamber showed that the dose would be too high to allow for safely working around the chamber, and additional shielding was needed. To resolve the issue, a sheet of lead was fashioned around the stainless steel tube that contains the Sr-90 source, making contact with the flanges on either end of the tube. The cavity between the tube and the lead sheet was filled with lead shot. Together, this added an additional 0.71 inches of lead shielding. The additional shielding successfully eliminated nearly all of the remaining X-ray radiation. Tables 3.3 and 3.4 summarize the path of radiation as shown in Figure 3.2, the thicknesses of each shielding material for each path, and the attenuated dose rates.

**Table 3.3** – Thickness of shielding materials along various paths through the source housing and SraT chamber.

Path	Path Lengths			
	Graphite (cm)	Tungsten (cm)	Stainless steel (cm)	Lead (cm)
A	0.318 ± 0.05	0.953 ± 0.05	0.401 ± 0.05	1.803 ± 0.05
B	0.419 ± 0.05	0.782 ± 0.05	0.401 ± 0.05	1.803 ± 0.05
C	1.523 ± 0.05	1.854 ± 0.05	0.635 ± 0.05	0.00
C'	0.305 ± 0.05	1.143 ± 0.05	0.635 ± 0.05	0.00
D	0.508 ± 0.05	0.965 ± 0.05	1.067 ± 0.05	0.00
D'	0.305 ± 0.05	3.81 ± 0.05	1.067 ± 0.05	0.00
E	0.305 ± 0.05	0.864 ± 0.05	0.401 ± 0.05	1.803 ± 0.05
F	0.508 ± 0.05	0.762 ± 0.05	0.401 ± 0.05	1.803 ± 0.05
G	0.00	0.00	0.00	0.00
H	0.787 ± 0.05	0.00	0.533 ± 0.05	1.981 ± 0.05
I	0.508 ± 0.05	0.762 ± 0.05	0.762 ± 0.05	2.54 ± 0.05

**Table 3.4** Left) Preliminary dose rates calculated by RadPro Calculator and (right) predicted attenuated dose rates through shielding materials along various paths.

	Exposure Position	Storage Position
Path	Preliminary dose rate (d) (mR/hr)	Attenuated dose rate (D) (mR/hr)
A	81.0 ± 0.05	15.4 ± 3.09
B	98.0 ± 0.05	18.6 ± 3.75
C	1.7 ± 0.05	1.3 ± 0.38
C'	2.2 ± 0.05	1.6 ± 0.49
D	6.5 ± 0.05	4.0 ± 1.89
D'	0.17 ± 0.05	0.1 ± 0.066
E	90.0 ± 0.05	17.1 ± 3.44
F	135.0 ± 0.05	25.7 ± 5.16
G	822000.0 ± 0.05	-
H	116.0 ± 0.05	18.6 ± 4.75
I	105.0 ± 0.05	11 ± 3.86

The preliminary dose rate is the dose rate just outside of the source housing. These values were calculated by RadPro Calculator. The attenuated dose rate column represents the predicted dose rates directly outside of the shielding materials. Because radiation falls off as  $\frac{1}{r^2}$  with distance outside of the shielding, employee dose will be much lower than these values.

# Chapter 4

## Results and Analysis

This section analyzes the predicted dose rate values by applying them to a theoretical accumulated dose scenario to predict employee dose over time. Employee dose predictions fall far below safe dose limits. Comparison of the predicted dose rates to actual measured dose rates after installation of the Sr-90 source are made. Measured values verify that proper shielding is in place and that predicted values for dose rate were calculated correctly. Error in calculation of predicted rates will be discussed.

### 4.1 Accumulated Dose Scenario

The values for predicted dose outside of the test chamber are very minimal. The largest value (800 Rad/hr) is the dose rate received by the unshielded samples directly under the beam of radiation inside of the chamber. As predicted in Table 4, the largest dose rate employees will experience outside of the shielding is about 25 mR/hr along path F (and this is if they are directly touching the chamber). Dose rate falls off as  $\frac{1}{r^2}$  with distance from the chamber. On average, the type of work involved with using SST chamber allows employees to be a distance of at least 50 cm from the test chamber, reducing the largest external dose rate to about 10 mR/hr. As a worst case scenario, if the

employee placed their hand on the outside of the SRaT chamber for the entire work day (8 hours), they would only receive a total of 200 mR. In order to receive the legal dose limit for extremities (50 rem), the employee would need to be in direct contact for a continuous 83 days. Background radiation measured in the building in which the test chamber resides is about 7 mR/hr. Thus, at distances of about 20 cm from the SraT chamber, the dose rate is at background.

## **4.2 Theoretical vs. experimental dose rates**

Upon installing the Sr-90 source into the SRaT chamber, a Radiation Safety Officer (RSO) made dose rate measurements near the chamber using a Geiger-Muller meter. This device is particularly well-suited for measuring X-ray counts per unit time.

Measurements were made along various paths as described in Table 4. Because the source was required to be installed by an RSO, I was not able to directly measure the dose rates or the distances they were taken from. I was required to stand some distance away during the procedure. As the RSO called off the reading of each measurement made, I wrote down the dose rate value and estimated the distance from the source to the detector. Figure 4.1 compares the predicted values of attenuated dose rate to the actual measured values of dose rate using the Geiger-Muller meter. The error bars are large primarily due to the uncertainty in the distance to the detector.

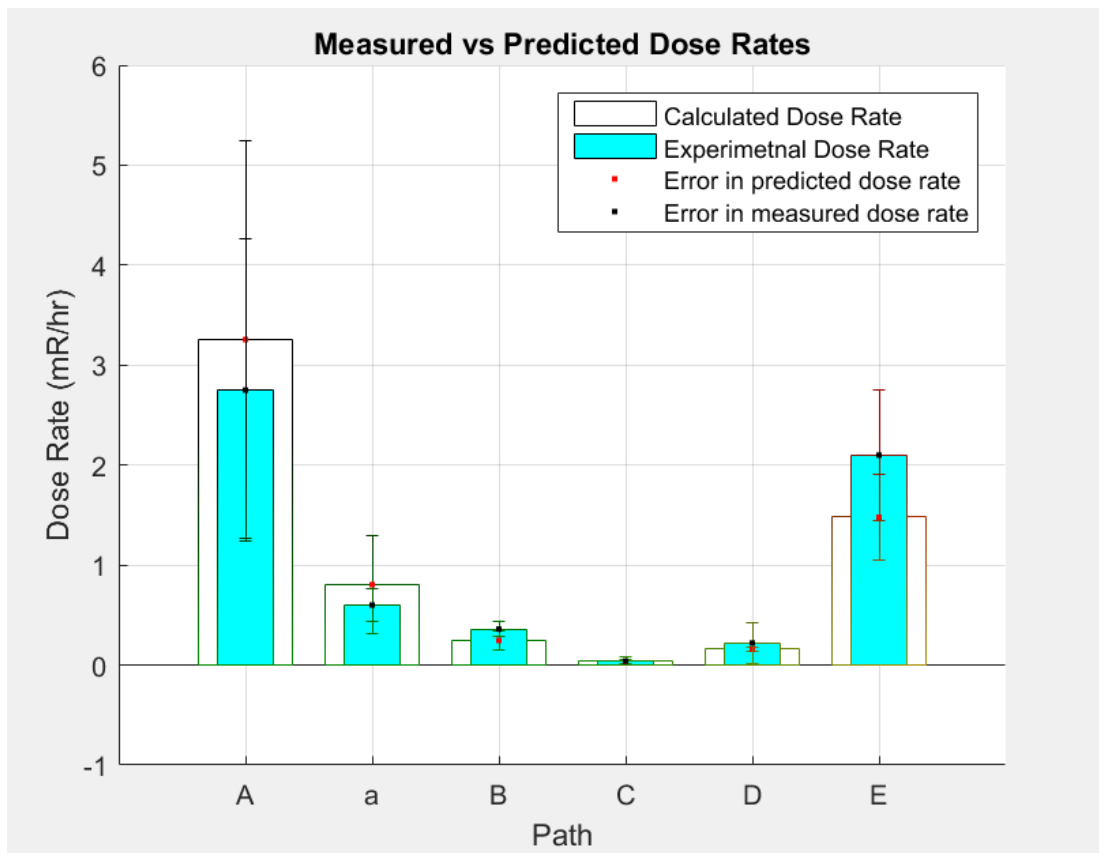


**Figure 4.1** Predicted attenuated dose rates vs. measured dose rates.

Measurements were not made along all of the predicted paths. A description of the paths along which measurements were made and the percent difference between predicted and measured values along those paths are as follows (refer to Figure 3.2 for path orientation).

Path	Direction	% Difference	Average % Difference
Path A	~10 cm above unshielded source housing	16.86	26.72
Path a	~10 cm above shielded source housing	29.07	
Path B	~20 cm below shielded source housing	37.63	
Path C	~20 cm toward pillow block	10.52	
Path D	~15 cm away from the housing end cap	31.58	
Path E	~2 cm outside of Pb shielding	34.68	

The error bars of both the predicted and calculated dose rates fall within in each other. Thus, the predicted attenuated dose rate is well correlated to the actual measured values of dose rate. Although measurements were not made along every predicted path, we assume that the predicted values along those paths were also calculated correctly.

Although the uncertainty has about the same magnitude as the values of dose rate, if we consider the highest value of error, the X-ray dose rate one would receive is only a little over 5 mR/hr. In order to receive this dose rate, the employee would have to be working directly above the shielded source at a distance of about 10 cm. The setup of the SST chamber makes this completely unnecessary and avoidable. The miniscule dose rate received at a conservative distance of 50 cm from the source would allow employees to work safely around the SST chamber without concern.

### **4.3 Error Analysis**

This section describes the method of calculating error in the predicted dose rate values. The equation for dose rate is formulated and the standard deviation for each data point is calculated.  $\chi^2$  is found for the data. Error is then propagated into experimental dose rate values. Predicted dose rate is plotted against measured dose rate with their relative error bars.

#### **4.3.1 Dose Rate Equation**

Assuming linear attenuation, the attenuation factor  $\xi$  (equation 3) for lead (Pb) and stainless steel (Fe) can be calculated at the minimum and maximum X-ray energies as

$$\xi_{Pb_i} = e^{-\frac{x_{Pb}}{L_{Pb_i}}}$$

$$\xi_{Pb_j} = e^{-\frac{x_{Pb}}{L_{Pb_j}}}$$

$$\xi_{Fe_i} = e^{-\frac{x_{Fe}}{L_{Fe_i}}}$$

$$\xi_{Fe_j} = e^{-\frac{x_{Fe}}{L_{Fe_j}}}$$

where  $i$  is the minimum energy 0.5 MeV, and  $j$  is the maximum energy 2.5 MeV. The attenuation of each material is simply an average attenuation at the minimum and maximum energies

$$\xi_{avg_{Pb}} = \frac{\xi_{Pb_i} + \xi_{Pb_j}}{2}$$

$$\xi_{avg_{Fe}} = \frac{\xi_{Fe_i} + \xi_{Fe_j}}{2}$$

Together, the lead and stainless steel shielding provide a combined average attenuation factor

$$\xi_{avg} = \xi_{avg_{Pb}} \cdot \xi_{avg_{Fe}}$$

The attenuated dose rate  $D$  is now simply the preliminary dose rate  $d$  multiplied by this attenuation factor

$$D = d \xi_{avg} \quad (4)$$

### 4.3.2 Standard Deviation of Attenuated Dose Rate

The uncertainty in scattering length and thickness for the lead and stainless steel shielding is summarized below.

Material	$\sigma_{L_{0.5MeV}} (cm)$	$\sigma_{L_{2.5MeV}} (cm)$	$\sigma_x$
Lead (Pb)	0.2	0.2	0.1
Stainless steel (Fe)	0.2	0.2	0.1

This equation for  $D$  along with these values are used to find the standard deviation of the calculated attenuated dose rates. The standard deviation  $\sigma D$  was calculated by adding error in quadrature of equation 4.

$$\sigma D = \left[ \sigma d^2 \left( \frac{\partial}{\partial d} D \right)^2 + \sigma L_{Fe_i}^2 \left( \frac{\partial}{\partial L_{Fe_i}} D \right)^2 + \sigma L_{Fe_j}^2 \left( \frac{\partial}{\partial L_{Fe_j}} D \right)^2 + \sigma L_{Pb_i}^2 \left( \frac{\partial}{\partial L_{Pb_i}} D \right)^2 + \sigma L_{Pb_i}^2 \left( \frac{\partial}{\partial L_{Pb_i}} D \right)^2 + \sigma x_{Fe}^2 \left( \frac{\partial}{\partial x_{Fe}} D \right)^2 + \sigma x_{Pb}^2 \left( \frac{\partial}{\partial x_{Pb}} D \right)^2 \right]^{\frac{1}{2}}$$

Predicted attenuated dose rates with their relative error along each path are represented in Figure 4.2 (refer to Figure 3.2 for path orientation). Because it is unshielded, path G was excluded due to its large magnitude compared to the other data points. Plotting G hinders seeing the size of other values because their relative magnitude are small compared to G, even when plotted logarithmically.

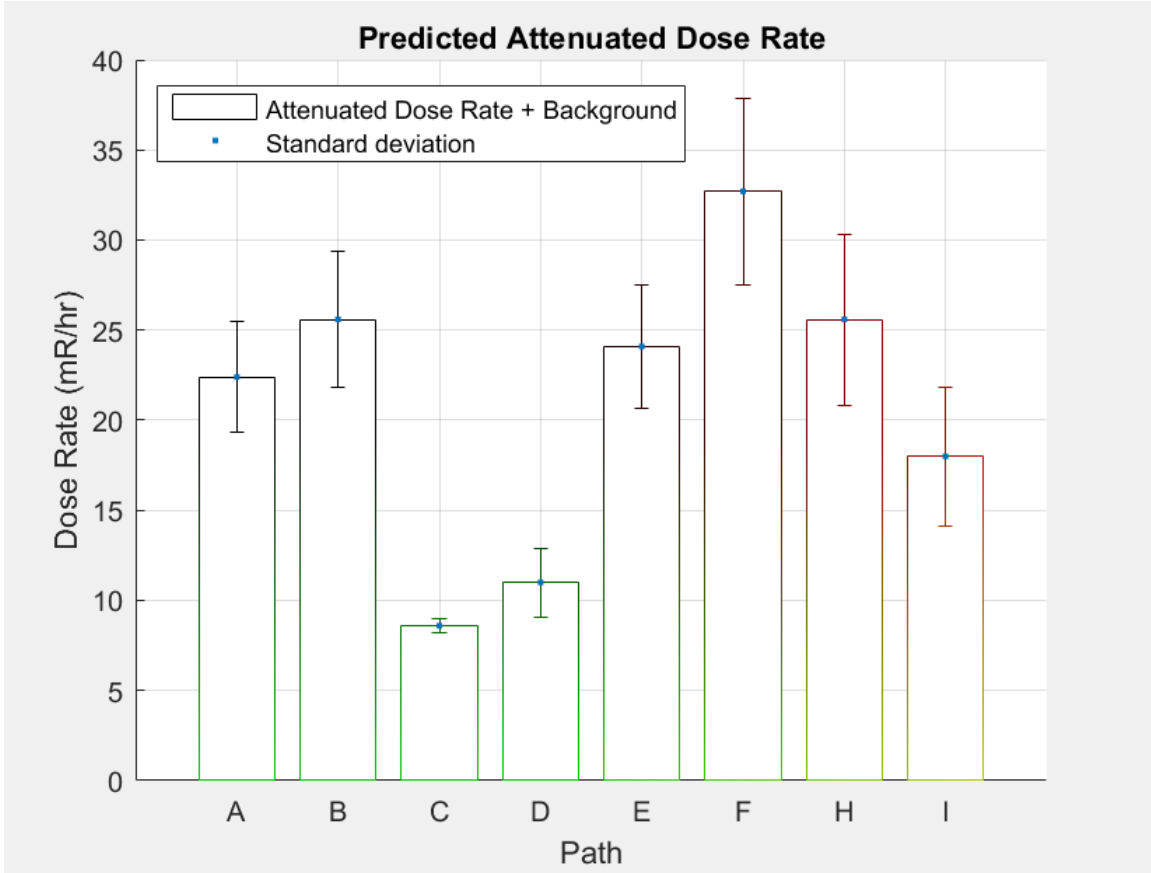


**Figure 4.2** Predicted attenuated dose with standard deviation.

### 4.3.3 Calculating $\chi^2$

The  $\chi^2$  value for the predicted attenuated dose rates against the actual measured values was calculated as

$$\chi^2 = \sum \left( \frac{(MD - CD)^2}{\sqrt{(\sigma_{CD})^2}} \right)$$

Where  $MD$  is the measured dose rates,  $\sigma_{MD}$  is the error in  $MD$ , and  $CD$  is the calculated dose rates. This calculation provides

$$\chi^2 = 10.03$$

The reduced  $\chi^2$  value is

$$\chi_v^2 = 1.67$$

The  $\chi^2$  value is about the number of data points (Figure 4.2), which provides a good argument that the calculated dose rates are well correlated with the actual measured values.  $\chi_v^2$  is close to the value of 1, which is also a good indicator that the predicted values fit the measured data.

# Chapter 5

## Conclusion

A safe test system for simulating high energy electron flux was developed. In order to ensure employee radiation dose remains within legal and safe limits, predictions of attenuated dose rates from the shielded Sr-90 source were calculated. The predicted values for X-ray dose rate through various shielding materials correlated with measured values post installation. Predicted values were thus calculated correctly and reflect the actual dose rate. Dose rates escaping the tests chamber through the shielding are low enough to allow employees to safely work around the source for extended periods of time. Incorporation of the Sr-90 source has diversified the Space Survivability Test chamber by allowing simulation of high energy electron radiation akin to geostationary orbit.

# Bibliography

- [1] Katie Gamaunt, Heather Tippets, Alex Souvall, Ben Russon and JR Dennison, “The Space Survivability Test Chamber,” *American Physical Society Four Corner Section Meeting*, Arizona State University, Tempe, AZ, October 16-17, 2015. *Presentation received award for outstanding Undergraduate Poster.*
  
- [2] Xinlin Li, D. N. Baker, M. Temerin, G. Reeves, R. Friedel, C. Shen  
*“Energetic electrons, 50 keV – 6 MeV, at geosynchronous orbit: their responses to solar wind variations”.*
  
- [3] Alex Souvall, Greg Wilson, Katie Gamaunt, Ben Russon, Heather Tippets and JR Dennison, “Properties of Spacecraft Materials Exposed to Ionizing Radiation,” *American Physical Society Four Corner Section Meeting*, Arizona State University, Tempe, AZ, October 16-17, 2015.
  
- [4] ASTM F1892, “*Standard Guide for Ionizing Radiation (Total Dose) Effects Testing of Semiconductor Devices*,” ASTM International, West Conshohocken, PA, 2012

- [5] JR Dennison, “*The Dynamic Interplay Between Spacecraft Charging, Space Environment Interactions and Evolving Materials*,” Abstract 125, Proceedings of the 13th Spacecraft Charging Technology Conference, (Pasadena, CA, June 25-29, 2014), 8 pp.
- [6] JR Dennison, John Prebola, Amberly Evans, Danielle Fullmer, Joshua L. Hodges, Dustin H. Crider and Daniel S. Crews, “*Comparison of Flight and Ground Tests of Environmental Degradation of MISSE-6 SUSpECS Materials*,” Proceedings of the 11th Spacecraft Charging Technology Conference, (Albuquerque, NM, September 20-24, 2010), 12 pp.
- [7] Robert H. Johnson, Lisa D. Montierth, JR Dennison, James S. Dyer, and Ethan Lindstrom, “*Small Scale Simulation Chamber for Space Environment Survivability Testing*,” IEEE Trans. on Plasma Sci., 41(12), 2013, 3453-3458.  
DOI: 10.1109/TPS.2013.2281399
- [8] Greg Wilson, Ben Russon, Alex Souvall, Katie Gamaunt, Heather Tippets, Lisa Phillipps, JR Dennison, and James S. Dyer, “*Small Satellite Materials and Components Space Survivability Assessment with Space Environments Effects Test Facility*,” 30th Annual AIAA/USU Conference on Small Satellites, (Logan, UT, August 8-13, 2016).
- [9] Amberly Evans and JR Dennison, “*The Effects of Surface Modification on Spacecraft Charging Parameters*,” IEEE Trans. on Plasma Sci., 40(2), 291-297 (2012). DOI: 10.1109/TSP.2011.2179676

- [10] Edward R. Long, Jr., “*Electron and Proton Absorption Calculations for Graphite/Epoxy Composite Model*”, NASA Technical Paper 1568, Scientific and Technical Branch (November, 1979).
- [11] JR Dennison, James S. Dyer, J. Duce, J. Hodges, J.W. Burns, C.D. Thomson, L. Pearson, L. Davis, and R.S. Hyde, “*The State of Utah Space Environment & Contamination Study (SUSpECS) MISSE-6 Experiment*,” 1st Annual USU Space Dynamics Laboratory IR&D Enabling Technologies Demonstration Day, Logan, UT, July 14, 2006.